Noname manuscript No.
(will be inserted by the editor)

A dual-permeability model for anomalous moisture transport in cement-based materials

Zhidong Zhang · Ueli Angst

Abstract Anomalous moisture transport in cement-based materials is often reported in the literature, but the conventional single-porosity moisture transport models generally fail to provide accurate simulation results. The present study proposes a dual-permeability model based on the dual-porosity concept, which includes the contribution of both liquid water and water vapor. The volumetric fraction of each porosity region is determined when fitting the measured sorption isotherms by using a bimodal equation. The validation with experimental data shows that the dual-permeability model can well simulate both the "normal" and the anomalous moisture transport. The applicability of the proposed model implies that the "dual-porosity property" could be one of reasons that cause anomalous moisture transport in cement pastes. In addition, we found that the vapor diffusion can be neglected for both porosities at high relative humidity (RH), while for low RH, it is not negligible.

Keywords van Genuchten-Mualem model · water vapor sorption isotherm · moisture transfer factor · volumetric fraction · cementitious materials

1 Introduction

The durability of reinforced concrete structures is closely related to moisture state in concrete [1]. Aggressive agents (e.g. chloride) can penetrate into concrete with liquid water (e.g.,[2,3,4,5,6]). When concrete is unsaturated, carbon dioxide (CO_2) can rapidly diffuse in the pores that are not filled with liquid water. These processes are able to cause corrosion of the reinforced steel (rebar) and deterioration of concrete structures [7]. Therefore, appropriate moisture transport models are essential for the predication of structures durability. Conventionally, a moisture transport model based on the Darcy's or Fick's law is used

Z. Zhang
Institute for Building Materials (IfB), ETH Zurich, 8093 Zurich, Switzerland
Tel.: +41 44 633 77 05
E-mail: zhangzhi@ethz.ch

U. Angst
Institute for Building Materials (IfB), ETH Zurich, 8093 Zurich, Switzerland
Tel.: +41 44 633 40 24
E-mail: ueli.angst@ifb.baug.ethz.ch

to predict the moisture state in cement-based materials (e.g., [8,9,10]). However, concerning anomalous moisture transport reported in the literature (e.g., [11,12,13,14]), the conventional models fail to predict the mass change of a specimen.

Anomalous moisture transport is found in both water uptake and drying of the cement-based materials. Hall and his colleagues considered an anomalous process as that the measured mass change curve (Δm vs. square root of time $t^{1/2}$) does not obey the linear relation [12,13]. When the moisture transport occurs in the hygroscopic range, the case that the measured mass change (loss or increase) curves do not follow the curves calculated by Fick's law has been termed as anomalous moisture transport [11]. Recently, Saeidpour and Wadsö [14] reported anomalous mass change curves when cement paste samples were subject to drying/wetting in a Dynamic Vapor Sorption (DVS) analyzer.

Anomalous moisture transport can result from various reasons. The generally considered ones are:

1. Complex pore structure. Cement-based materials have a broad pore size distribution, ranging from micropores (nm size) to macropores (μm and mm size), which are classified as large and small capillary pores, gel pores, and interlayer pores [15]. Nevertheless, most of the moisture transport models are developed on the basis of the single-porosity concept, meaning that transport properties in different sizes of pores are not distinguished. The concept of dual-porosity to explain anomalous moisture transport in cementitious materials was introduced in [16] and the calculated curves successfully captured the shapes of various anomalous mass loss curves.
2. Chemical interactions of water with hydration products. For liquid water uptake, Hall et al. [12] argued that the anomalous water absorption in cement-based materials is caused by re-hydration of unreacted cement and dehydrated components of hardened cement pastes. Zeng and Xu [17] also assumed reaction kinetics occurring along with moisture transport in cement pastes and employed a fractional kinetic model to represent anomalous drying.
3. Dimensional changes. The macroscopically observed drying shrinkage is induced by the microscopic damages of pores due to the relatively large capillary force established during water evaporation. The swelling associated with the water uptake was observed by either the environmental scanning electron microscope (ESEM) [12] or nuclear magnetic resonance (NMR) [18]. Both shrinkage and swelling result in the changes of pore structures. The effect of microstructural alterations on moisture transport is not considered by the moisture transport models in the literature.
4. Moisture interactions with the surrounding environment. The moisture interactions between the porous material and the environment depend on many factors, such as ambient RH, material moisture state, porosity and pore size at the surface, etc. The general models use the constant evaporation rate to represent the complicated moisture interactions (e.g., [19]), which definitely ignores some important factors.

The present study aims at evaluating whether the complex pore structure could be one of reasons for anomalous moisture transport. The complex pore structures are represented by the dual-porosity concept and moisture transport in different porosities is considered by introducing a dual-permeability model.

2 The dual-porosity/dual-permeability concept

The dual-porosity/dual-permeability concept is widely used in geoscience for simulating mass transport in soils and fractured media (e.g. [20,21,22,23]). It was also adapted to other porous materials, such as food [24] and coal [25]. The concept of dual-porosity/dual-permeability model was originated from the study of Barenblatt et al. [20] on saturated water flow in fissured rocks. In that work, the natural fracture network and the intact rock matrix were simulated as two overlapping porous media with their own porosity, permeability, and fluid pressure fields, and the water flow was fulfilled by Darcy's law with the transfer of liquid between the fissures and the pores. Most of the subsequent dual-permeability models followed the same concept as Barenblatt et al. [20]. These models contain three permeabilities: one for the fracture, one for the matrix and one for the fracture-matrix interface. The latter one describes the exchange of flows at the interface of the two porous regions. In the simplified dual-porosity model (no flow in the matrix) proposed by Warren and Root [21] for naturally fractured media, they treated the flux at the interface proportional to the pressure difference in these two regions. In a popular model for unsaturated porous materials, Gerke and van Genuchten [26,27] calculated the interface permeability as the mean of permeabilities of matrix and fracture. In this model, Richards' equation was used to govern water flow in both regions. Two water retention curves, one for the matrix and one for the fracture, were formulated by van Genuchten (VG) equation [28] and the relative permeabilities were calculated by the van-Genuchten-Mualem (VGM) equation [28,29]. Since then, this set of equations were commonly found in the literature for modeling unsaturated moisture transport in porous media [30,31,32,33].

The application of dual-porosity/dual-permeability models to cement-based materials is only found in a few studies. Carlier and Burlion [34] and Zhang et al. [35] borrowed the dual-porosity concept and used the bimodal equation proposed by Durner [36] to fit the measured sorption isotherms. They found that the use of the bimodal equation could show much better agreements between experimental data and theoretical curves, especially for extremely high and low degrees of saturation. Nevertheless, the uncertainty of fitting is higher because of more undetermined parameters in the bimodal equation. Recently, Smyl et al. [33] used a dual-permeability modeling approach to simulate water flow in fractured cement-based materials with micro-cracks. A new equation for the water transport coefficient across matrix-fracture interface was proposed to take into account permeabilities of both regions. Their simulation results showed that the classical model failed to adequately describe the long-term water ingress in fractured materials, whereas the dual-permeability model well simulated moisture transport in late stages of water ingress.

When adapting the dual-permeability model from geoscience to cement-based materials, we must know that (1) the moisture transport mechanisms in materials with fine pores such as cement-based materials are different from soils (granular materials) or rocks (fractured media), and (2) the volumetric fraction of each region is not directly measurable for the undamaged cement-based materials. Concretes in the natural condition are often unsaturated; thus, a moisture transport model should consider two phases at least, liquid and vapor [10,37]. For soils or fractured media, the volumetric fraction of each region can be estimated from the aggregate-macropores ratio [26,30,31] or the measured volume of the fracture system [38]. The volumetric fraction of fracture in damaged concrete was experimentally determined with

a microscope [33]. However, it is very often found that the boundary between two porosity regions is arbitrarily chosen in the literature with vague criteria [39]. For these cases, the volumetric fraction was set as a free parameter (e.g., [32]) and determined by fitting the experimental data. In regard to undamaged cement-based materials, it is not easy to determine the volume for each porosity region since there is no a clear boundary between two regions.

To tackle these issues for cement-based materials, the present study proposes a two-phase moisture transport model (e.g., [10, 19]) for the dual-permeability modeling and the volumetric fraction is determined when fitting the measured sorption isotherms by using a bimodal equation [36]. Experimental data for anomalous moisture transport, measured by a DVS instrument [14], are used to validate the proposed modeling approach.

3 Applying the dual-permeability concept to cement paste

3.1 Structure of cementitious materials

When cement is mixed with water, hydration products (mainly calcium-silicate-hydrate, C-S-H) immediately grow from the surfaces of the cement particles. Initially, the flake-like structure appears and eventually hydration products become the needle-like structure [40]. The impingement of hydration products from the adjacent cement grains creates a pore network composing of various sizes of pores. If simply separating these pores into two groups with large and small pores, the hydrated cement paste can be viewed as a dual-porosity material with two regions, large pore region and small pore region. We assume that pores in each region are well connected, meaning that fluids can move in each region, as well as communicate between two regions. This indicates that definitions of large and small pores in this study are mainly based on the moisture transport properties in pores. For this case, two regions cannot be separated by a single value of pore size because this boundary between two regions varies with the moisture transport properties. This is why in this study terms like "large" and "small" pores are used, other than "macropore" and "micropore" or "capillary" and "gel" pores because there terms always imply that pores in two regions are in a fixed pore size range.

The porosity and degree of saturation of each region can thus be determined based on the dual-porosity concept. Volumes occupied by different phases for a material with two porosity regions are illustrated in Fig. 1. Let us define the total porosity ϕ of a cement paste as the total pore volume V_p per unit volume of the material V_t; that gives $\phi = V_p/V_t$. Similarly, porosities of the large and small pore regions are defined as $\phi_l = V_{p,l}/V_t$ and $\phi_s = V_{p,s}/V_t$ (see illustrations in Fig. 1). Then, we have $\phi = \phi_l + \phi_s$.

The degree of saturation S in each region is calculated according to Fig. 1. S for each of them is written as $S_l = V_{w,l}/V_{p,l}$ and $S_s = V_{w,s}/V_{p,s}$, respectively. The total degree of saturation is

$$S = \frac{V_{w,l}}{V_{p,l} + V_{p,s}} + \frac{V_{w,s}}{V_{p,l} + V_{p,s}} \tag{1}$$

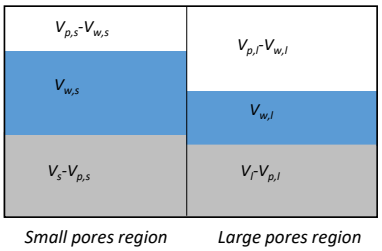

Fig. 1 Definition of porosity in a material with two porosities. Abbreviations are: s=small pores, l=large pores, w=water occupied volume, and p=pores occupied volume.

If defining the volumetric fraction of large pore region as $w_f = V_{p,l}/(V_{p,l} + V_{p,s})$, the total degree of saturation is rewritten as

$$S = w_f S_l + (1 - w_f) S_s \tag{2}$$

Thus, porosities of the large and small pores regions are calculated by

$$\phi_l = w_f \phi; \quad \phi_s = (1 - w_f)\phi \tag{3}$$

Note that the definition of w_f is different from that in Gerke and van Genuchten [27] which included the volume of non-porous solid phase. Assuming no solid in the large pore region ($V_l = V_{p,l}$), w_f should be multiplied by the total porosity ϕ to give the same value as that in [27].

3.2 Mass exchange between two porosity regions

As mentioned above, both linear and non-linear mass transfer between the large pores and small pores were studied in the literature for the fractured media. It has been shown that the linear mass exchange was able to accurately represent the mass exchange between two porosity regions [26], which is written as:

$$\Gamma_w = \beta_w (RH_s - RH_l) \tag{4}$$

where β_w (kg/s/m^3) is the first-order rate coefficient, which is generally assumed to be dependent on the geometry of the small pore region, the length scale of the large pores region and permeability at the interface of two regions [26,27]. For concrete, Smyl et al. [33] let β_w be a function of the liquid conductivity in two porosity regions. In this study, we simplify the relation as the following expression.

$$\beta_w = \xi k_{r,l} k_{r,s} \tag{5}$$

where ξ (kg/s/m^3) is the moisture transfer factor and $k_{r,i}$ is the relative liquid permeability ($i = l$ or s).

Concerning the case of cement paste, the moisture transfer factor ξ is not directly measurable. In this study, we firstly let ξ be a free parameter that will be determined by fitting the mass change curve measured during drying/wetting tests and then find a value that works for all cementitious materials.

3.3 Determination of w_f based on measured sorption isotherm

For the single-porosity moisture transport model, a unimodal equation is able to describe the sorption isotherm. The most widely used one is the VG equation [28].

$$S = \left[1 + \left(\frac{P_c}{\alpha}\right)^{\frac{1}{1-m}}\right]^{-m} \tag{6}$$

where α (Pa) and m (-) are parameters determined by fitting the measured sorption isotherm and P_c (Pa) is capillary pressure.

A bimodal equation that is used for the dual-porosity model is obtained by applying the VG equation for each porosity region; therefore, Eq. (2) becomes

$$S = w_f \left[1 + \left(\frac{P_c}{\alpha_l}\right)^{\frac{1}{1-m_l}}\right]^{-m_l} + (1 - w_f)\left[1 + \left(\frac{P_c}{\alpha_s}\right)^{\frac{1}{1-m_s}}\right]^{-m_s} \tag{7}$$

Although the bimodal equation is able to provide a high fitting accuracy, the fitted parameters are subject to a relatively large uncertainty because of more parameters in the bimodal equation than the unimodal equation [34,35]. To decrease the uncertainty, one way is to reduce the number of parameters. In VG equation, the air-entry pressure related parameter α_i should be different for the large and small pores [41], but the shape parameter m was found in a very narrow range (0.4-0.5) for OPC pastes with water-to-cement ratios from 0.35 to 0.6 [35]. Our previous study suggested a constant value (0.45) for the studied OPC pastes [6]. Therefore, only three parameters in Eq. (7) need to be determined by fitting the measured sorption isotherm, namely, w_f, α_l, and α_s.

3.4 Transport model in unsaturated porous materials

Moisture transport in unsaturated porous media can be simulated by either multi-, two- or single-phase models as reviewed in [37]. For the general purpose of focusing on the mass change, a two-phase model, including the transport of liquid and vapor, is sufficient. The governing equations for the mass balance in 1D are written for the large and small pores as [42, 19]

$$\rho_w \frac{\partial S_l}{\partial t} = \frac{1}{\phi_l}\frac{\partial}{\partial x}\left(-\rho_w \frac{K_{w,l} k_{r,l}}{\eta}\nabla P_{w,l} - D_{v0} f_l \nabla \rho_{v,l}\right) + \frac{\Gamma_w}{\phi w_f} \tag{8}$$

$$\rho_w \frac{\partial S_s}{\partial t} = \frac{1}{\phi_s}\frac{\partial}{\partial x}\left(-\rho_w \frac{K_{w,s} k_{r,s}}{\eta}\nabla P_{w,s} - D_{v0} f_s \nabla \rho_{v,s}\right) - \frac{\Gamma_w}{\phi(1 - w_f)} \tag{9}$$

where ρ_w and $\rho_{v,i}$ (kg/m^3) are the densities of liquid water and vapor, respectively; $P_{w,i}$ (Pa) is the liquid pressure, η (Pa·s) represents the dynamic viscosity of liquid water, $K_{w,i}$ (m^2) is the liquid intrinsic permeability, D_{v0} (m^2/s) is the free vapor diffusion coefficient in the air, and $f_i = f_i(S_i, \phi_i)$ represents the resistance factor for vapor diffusion and is related to many factors, including porosity, water content, connectivity and tortuosity of the pore network.

The resistance factor in Eqs. (8) and (9) represents the reduction of accessibility for water vapor diffusion due to the presence of the solid and liquid phases, the tortuous path for diffusion, the different connectivities in the pore network, etc. Because of limited experimental results, the expression of $f_i(S_i, \phi_i)$ is generally derived from theoretical concepts. One equation that has been used for cement-based materials is given as [9,37]

$$f_i(S_i, \phi_i) = \phi_i \left(1 - S_i\right) \alpha(S) \tau_i \tag{10}$$

where $\phi_i \left(1 - S_i\right)$ is the space avaliable for vapor diffusion and $\alpha(S)\tau_i$ represents the tortuosity of the sole gaseous phase in the porous material and is written as [43]

$$\alpha(S)\tau_i = \phi_i^{x_D - 1} \left(1 - S_i\right)^{x_D + 1} \tag{11}$$

where parameter $x_D = 2.74$ as suggested by Thiéry et al. [44] for cement-based materials.

The relative permeability $k_{r,i}$ is a unique function of S_i and calculated by the well-known VGM equation [28,29].

$$k_{r,i}(S_i) = S_i^{0.5} \left[1 - \left(1 - S_i^{1/m}\right)^{m_i}\right]^2 \tag{12}$$

This moisture transport model assumes that the equilibrium between liquid and vapor within each porosity region is always fulfilled. At the equilibrium state, the relation between capillary pressure, P_c, and relative humidity, RH, is governed by Kelvin's law. Note that the equilibrium assumption is not valid between two porosity regions since mass exchange is always occurring if the pressure/RH difference exits. Unless, when a drying or wetting process reaches the mass equilibrium state, RH in the small pores becomes the same as that in the large pores and no mass exchange exits any more. Furthermore, the imposed boundary condition is used for all simulations to simply the model.

Overall, two intrinsic permeabilities ($K_{w,l}$ and $K_{w,s}$) and the moisture transfer factor (ξ) need to be calibrated by experimental data, such as the measured mass change curves and saturation profiles. The first two are from the moisture transport properties which control the "inner" moisture transport. The latter is used for the moisture exchange between the large and small pores and it can be viewed as a constant, which will show in this paper. Thus, $K_{w,l}$ and $K_{w,s}$ are two undetermined parameters in proposed dual-permeability model.

4 Experimental validation

To validate the proposed model for the undamaged cement paste, experimental data are collected from the literature. We start from the measured "normal" moisture transport that can be well simulated by a single-porosity model, and then move to anomalous moisture transport that cannot be modeled by the single-porosity model. This is able to prove the applicability of the dual-permeability model to the anomalous moisture transport.

4.1 "Normal" moisture transport

Experimental data were collected from [45,46,19]. Two cement pastes with water-to-cement (w/c) ratios 0.45 and 0.6 (denoted by P1 and P2) were made from the same OPC cement (CEMI 52.5, according to EN 197–1 European standard) and sealed in cylindrical plastic bottles for two years. Experimental data include sorption isotherms, drying mass loss curves and saturation profiles at the end of drying. Water vapour sorption isotherms were measured by the saturated salt solution method on small crushed samples [45]. Drying tests were conducted by putting the cylindrical specimens (10 cm long and 7 cm in diameter) in a desiccator with constant RH at 53.5%. The specimens were sealed by self-adhesive aluminium foil sheets, and only one side was open for moisture exchanges with the ambient environment. Saturation profiles were measured by the gamma-ray attenuation method at the end of drying tests [46]. Previous studies [19] showed that measured mass loss curves and saturated profiles of these two cement pastes can be well simulated by the single-porosity model with K_w as the only fitting parameter. In this section, the dual-permeability method is used for these two pastes as well to see if the proposed model is able to yield better results.

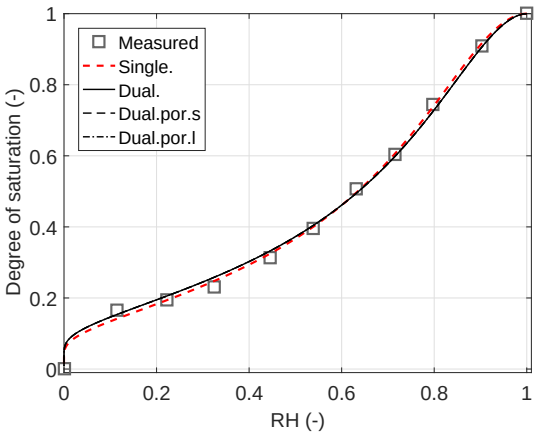

Fig. 2 Water vapor desorption isotherms for P1 paste. The fitted curves for large and small pores are identical, so they are hidden.

One example in Fig. 2 shows that the fitted sorption isotherms for P1 by the uni- and bi-modal equations (Eqs. (6) and (7)) are almost identical. For P2 paste (see the figure in the Supplementary Materials), the bimodal equation shows slightly better fitting than the unimodal equation which misses the curve shape at high RH, such as RH = 97%. The fitted w_f for P1 paste in Table 1 is greater than that for P2 paste. This is reasonable because the low w/c paste is supposed to have a higher volumetric fraction of small pores than the paste with high w/c.

Table 1 Parameters used in simulations for two pastes.

Paste	Model	$K_{w,s}(\mathrm{m}^2)$	$K_{w,l}(\mathrm{m}^2)$	ξ	w_f
P1	Single	1.75E-21		-	-
	Dual	9.71E-22	2.47E-21	1E-3	0.10
P2	Single	2.6E-20		-	-
	Dual	8.16E-21	1.08E-20	1E-3	0.16

Unlike the conventional models that only employed the measured mass change curves to calibrate parameters, the present study needs to get good results for both measured mass loss curves and saturation profiles. For instance, the sorption isotherms of large and small pores for P1 paste are identical, so to have good fitting of the measured mass loss curve, one could simply use the same value of $K_{w,l}$ as $K_{w,s}$. However, this would lead to a low fitting accuracy for the measured saturation profile because liquid permeabilities ($K_{w,i}k_{l,i}$) and vapor diffusion coefficients ($D_{v,0}f_i(S_i,\phi_i)$) are highly non-linear. Therefore, the calibration by two different sets of experimental data can provide more stable and robust results.

In addition, we found that when ξ is smaller than a certain value (1E-3 for P1 and 1 for P2), adjusting ξ does not improve fitting accuracy (see discussion in Section 5.1). Thus, ξ was assigned a value of 1E-3 kg/s/m^3 for all simulations. As the result, only two parameters ($K_{w,l}$ and $K_{w,s}$) are adjustable for simulations of the drying moisture transport in these two pastes.

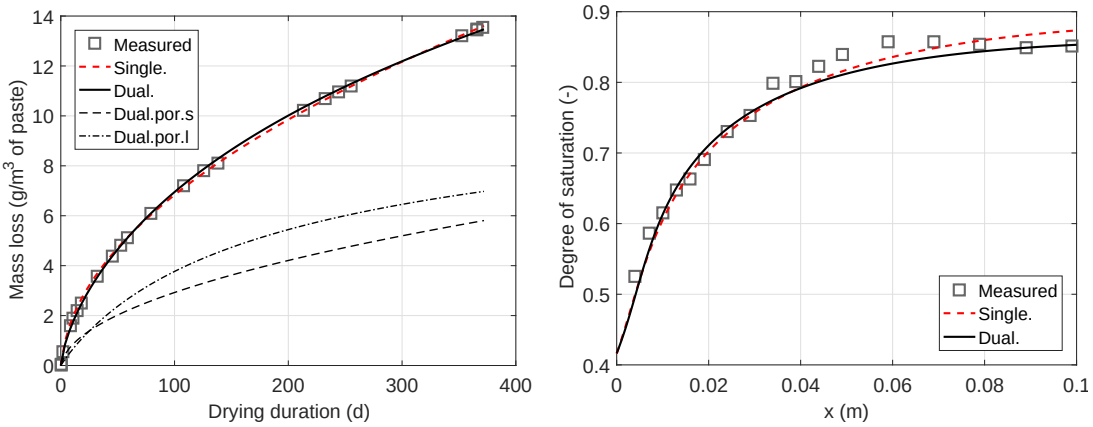

(a) Mass loss curves. (b) Saturation profiles at the end of drying.

Fig. 3 Measured and simulated mass loss curves and saturation profiles for P1 paste dried at RH=53%.

Simulation results for two cement pastes clearly show that both modeling methods, single-porosity and dual-permeability, provide very similar results for measured mass loss curves and saturation profiles (see Fig. 3 for P1 and figures in the Supplementary Materials for P2). For P1 paste, the mass loss from the small pores is higher than that from the large pores, which results from the high volumetric fraction of small pores. Regarding P2 paste, because of the sharp drop of sorption isotherm at high RHs for the large pores, the mass loss contribution of these pores is very low compared to the small pores.

4.2 Anomalous moisture transport

Data for anomalous moisture transport are mainly collected from [14], in which Type I OPC, supplied by HeidelbergCement® (different source from measurements in the previous subsection), with w/c=0.5, was used. The cylindrical specimens were cast in small stainless steel tubes (inner diameter 5.5 mm and sample length 2.0 mm) [47,14] and then were sealed for about 3 months. Drying and wetting tests were carried out on different specimens in a DVS 1000 (Surface Measurement System Ltd., UK). The sorption

isotherms, including desorption and adsorption, were measured on crushed samples in the same DVS [48]. The measured isotherms and data processing were reported in [37].

Since moisture distribution in the specimens during drying/wetting was not measured, parameters were only adjusted to fit the measured mass change curves. This can certainly induce uncertainties; thus, to reduce the number of parameters and to have more consistent results, ξ is kept at 1E-3 kg/s/m^3 for all simulations. Similar to the previous section, two parameters $K_{w,l}$ and $K_{w,s}$ are used to fit experimental data.

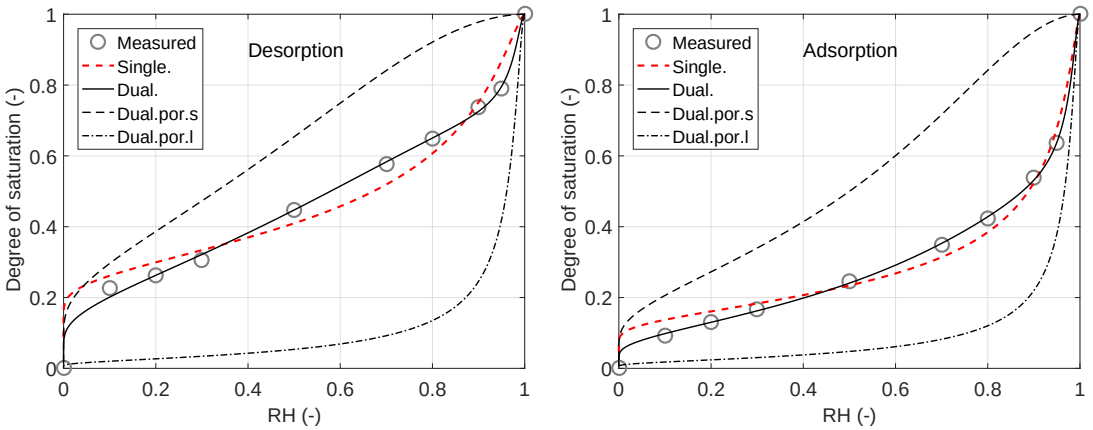

(a) Desorption isotherms. (b) Adsorption isotherms.

Fig. 4 Measured and fitted water vapor adsorption isotherms for the paste with anomalous moisture transport.

Table 2 shows that the fitted w_f for the desorption is lower than the adsorption. This is reasonable because during drying some large pores inside the material are blocked by the small pores due to the "ink-bottle" effect; therefore, moisture transport in these large pores behaves more like moisture transport in the small pores and do not contribute to moisture transport in the large pores.

Fitted sorption isotherms in Fig. 4 clearly show that the unimodal equation cannot provide accurate results for both desorption and adsorption isotherms because most of the measured points are not close to the calculated curves. The advantage of using the bimodal equation is that it largely increases fitting accuracy compared with the unimodal equation. Similar to the desorption curve for P2 paste, the sorption isotherms fitted by the bimodal equation for the large pores in Fig. 4 decrease sharply at the high RHs. This is expected due to the fact that liquid water in the large pores is removed quickly when the saturated sample is exposed to the unsaturated environment.

As the consequence of the less good fitting of the sorption isotherms, the simulated mass change curves by the single-porosity model cannot match the measured ones (see the red dashed curves in Figs. 5 and 6 and the other figures in the Supplementary Materials). Fig. 4 shows that the slope of the fitted desorption curve by the unimodal equation in the range of 70% - 90% RH is greater than that of the measured curve. As we know, the slope of a sorption isotherm is associated with the material's moisture capacity, which basically represents the amount of moisture that can be removed by drying. The greater slope means that more moisture, which is apparently much more than the measured mass loss, is expected to be removed

from the specimen when it reaches the mass equilibrium. Contrarily, the fitted adsorption curve by the unimodal equation in the range of 50% - 60% RH is gentler than the measured curve. As a result in Fig. 6, no matter how to adjust K_w, we could not make the calculated final mass by the single-porosity model increase close to the measured one. Because the calculated mass loss is much different from the measured one, the simulated curves become less sensitive to K_w.

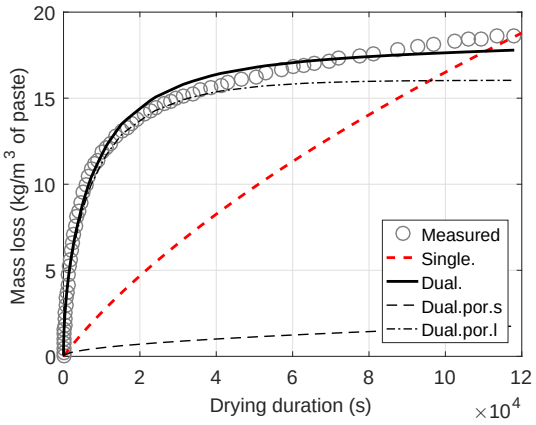

Fig. 5 Mass loss curves for OPC paste dried at RH=80% from initially 90%.

For simulations with the dual-permeability model, we have very good results which closely match measured curves. If comparing results in this study with the fitted curves in [16], it is clear that the analytical equation used in [16] (dual-Weibull distribution function) provides even higher fitting accuracy than the proposed dual-permeability model, but parameters in the analytical equation are not associated with any physical meanings. However, if the objective is to extrapolate the final mass of the specimen in the measurement of sorption isotherms, the dual-Weibull distribution function may be adequate. In addition, the analytical equation can be used for the specimen with irregular geometry, which is very common in practice (e.g., sorption isotherm measurements in a dynamic vapor sorption analyzer).

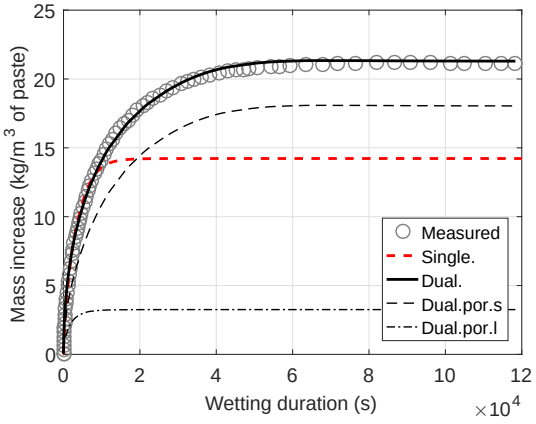

Fig. 6 Mass increase curves for OPC paste wetted at RH=60% from initially 50%.

The values of $K_{w,l}$ and $K_{w,s}$ in Table 2 show a scatter but if only comparing two drying (or wetting) cases, values of $K_{w,l}$ - the main contributor to moisture transport - are very close. Of course, we could not

find a set of $K_{w,l}$ and $K_{w,s}$ values that work well for both drying and wetting. This means that results from one drying/wetting condition may not be directly applicable to other conditions. Hence, the development of a universal dual-permeability model for all kinds of anomalous moisture transport need to consider more reasons as stated in the section of Introduction, such as chemical interactions of water with hydration products and the microstructural changes during drying/wetting.

When a single-porosity model is applicable, the dual-permeability model works as well, while the advantages of using a dual-permeability model are not significant. Therefore, we suggest that the dual-permeability model should be avoided for cases that a single-porosity model works. In other words, the first step to perform the dual-permeability simulations is to ensure that the studied material has two dual-porosity properties (more precisely, the large pore and the small pore regions as defined in Fig. 1). This can be done by checking if the measured sorption isotherm is well fitted with the unimodal equation. Otherwise, one can then try the dual-porosity/dual-permeability concept.

Table 2 Parameters obtained from fitting for anomalous moisture transport.

Cases	Model	$K_{w,s}$(m^2)	$K_{w,l}$(m^2)	w_f
Drying, RH 80%→70%	Single	1E-21		-
	Dual	5.35E-24	9.19E-19	0.345
Drying, RH 90%→80%	Single	1E-21		-
	Dual	2.44E-25	9.77E-19	0.345
Wetting, RH 50%→60%	Single	1E-18		-
	Dual	1.60E-21	4.31E-17	0.573
Wetting, RH 60%→70%	Single	1.2E-18		-
	Dual	6.43E-23	1.04E-17	0.573

5 Discussion

5.1 Effects of moisture transfer factor

The moisture transfer factor ξ controls the rate of moisture exchange between two regions. Examples in Fig. 7 show the effect of ξ on the moisture transport in two porosities. We can see that only when ξ is larger than a certain value the effect on moisture transport can be displayed in the mass change curves. This threshold value is case-dependent as shown in Fig. 7 that $\xi \approx$50 for drying and $\xi \approx$1E4 for wetting. These values are much greater than the one used for simulations (1E-3 kg/s/m^3). If let ξ be a free parameter for fitting, the value of ξ was found very low (around 1E-9 kg/s/m^3).

When cement-based materials are subjected to drying or wetting, RH in the large pores can reach to the same level with the boundary RH faster than in the small pores because of the greater transport coefficients in the large pores. Therefore, during drying, a greater mass transfer factor results in faster moisture being transferred from small pores to the large pores. Meanwhile, moisture in the large and small pores evaporates, so moisture in the small pores become less with the increase of ξ (see Fig. 7a). However, with more moisture accumulating in the large pores, it quickly evaporates to the environment because of the high transport coefficients of the large pores. This results in the stable moisture mass of the large pores but the higher total moisture loss from the specimen.

For wetting, a greater mass transfer factor can accelerate moisture condensation in the small pores from the large pores; this leads to more moisture increase in the small pore (see Fig. 7b). The high transport coefficients of the large pores ensure the stable moisture content in these pores. With the increase of moisture in the small pores, the total mass of the specimen increases as well.

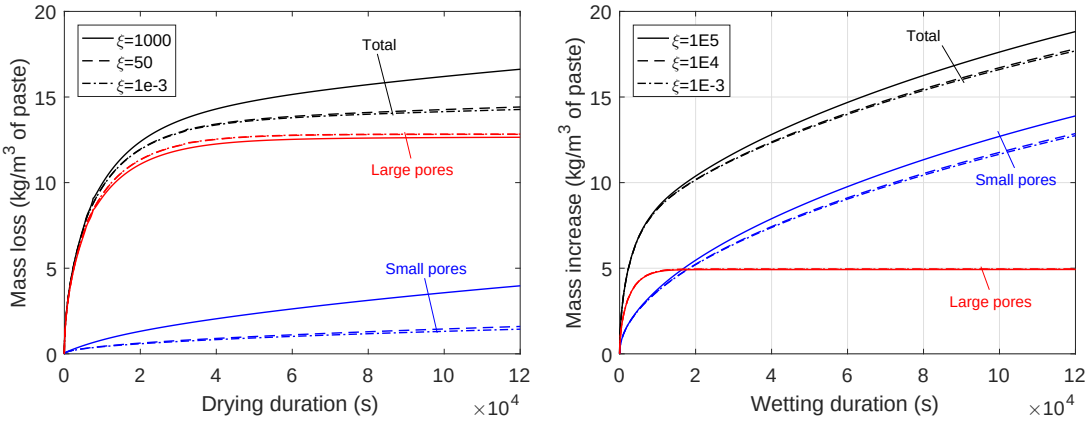

(a) Drying (b) Wetting

Fig. 7 Effect of mass transfer factor on moisture transport in the specimen and in small and large pores.

Fig. 7 indicates that If ξ is further increased, results show that moisture in small pores will be overdrawn for drying and overfilled for wetting. Therefore, large ξ must be used with caution because it may cause unrealistic simulation results. Unless, there are firm experimental evidence showing the great moisture transfer between the large and small pores. In this study, the low value of ξ was found to best agree with the experimental data.

5.2 Influence of vapour diffusion

In most dual-permeability models, vapor diffusion is not considered (e.g., [20,27,30,31,32,33]). Here, we investigate if vapor diffusion is indeed negligible in the case of dual-permeability simulations. Two simulations without including the vapor diffusion term in Eqs.(8) and (9) were performed by taking two drying tests of anomalous moisture transport as examples. Results displayed in Fig. 8 show that the ignorance of vapor diffusion has a slight effect on drying at RH=80%, whereas it greatly reduces the mass loss of drying at RH=70%. This may imply that for drying at low RHs the contribution of vapor diffusion is not negligible.

The contribution of each phase (liquid or vapor) to the moisture transport can be assessed by calculating the apparent diffusivity D_a considering the moisture transport as a pure diffusion-like process. Based on Eqs. (8) and (9), D_a for each porosity system is written as

$$D_{a,i} = k_{r,i}\frac{K_{l,i}}{\phi_i \eta_l}\frac{\mathrm{d}P_{c,i}}{\mathrm{d}S_i} + \left(\frac{M_v}{\rho_l RT}\right)^2 D_{v0} f_i(S_i,\phi_i)\frac{P_{vs} RH_i}{\phi}\frac{\mathrm{d}P_{c,i}}{\mathrm{d}S_i} \tag{13}$$

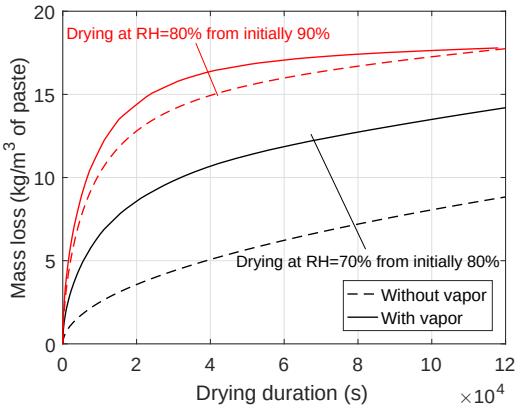

Fig. 8 Importance to consider vapor diffusion in the dual-permeability model.

The total D_a for a material with dual-porosity is estimated by a similar equation to the degree of saturation (Eq.(2)).

$$D_a \approx w_f D_{a,l} + (1 - w_f) D_{a,s} \tag{14}$$

By using the determined $K_{w,s}$ and $K_{w,l}$ from drying at RH=80% in Table 2, the calculated $D_{a,s}(RH)$ and $D_{a,l}(RH)$ curves are shown in Fig. 9. The $D_{a,l}(RH)$ curve is always above the $D_{a,s}(RH)$ curve as permeability for large pores is much greater than that for the small pores. Fig. 9 reveals that the moisture contribution of each phase varies with RH. The lowest points of $D_{a,s}(RH)$ and $D_{a,l}(RH)$ curves, which is considered as the demarcation between the liquid and vapor transport dominant regions, are at 50% and 74%, respectively. This agrees with the fact that liquid water in the small pores is less affected at high RH than that in the large pores. The comparison of mass loss for two drying cases in Section 4.2 shows that mass loss in the small pores for drying at 70% RH becomes less than that for drying at 80% RH. It needs lower RH to remove or disconnect liquid water in the small pores. At the lowest point of the $D_a(RH)$ (RH=70% in Fig. 9), the contribution for liquid water and vapor is comparable. This is the reason that Fig. 8 shows the non-negligible fraction of mass loss from vapor diffusion for drying at 70% RH.

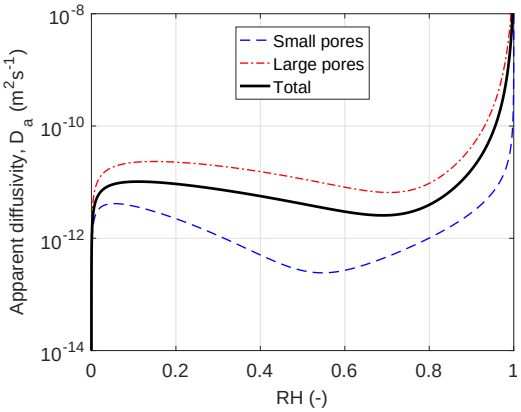

Fig. 9 Calculated apparent diffusivity D_a (taking the case of drying at RH=80% as an example).

5.3 The overall permeability

Based on the determined intrinsic permeabilities for two porosity regions, the overall intrinsic permeability of a cement paste K_w is often calculated by the following equation in the literature (e.g., [27,33]).

$$K_w = \phi w_f K_{w,l} + \phi(1 - w_f)K_{w,s} \tag{15}$$

To verify this equation, $K_{w,l}$ and $K_{w,s}$ of P1 and P2 pastes are chosen to calculate K_w, because both single-porosity and dual-permeability models provide accurate fitting for these two pastes. The calculated K_w are 4.6E-22 and 4.2E-21 m^2 for P1 and P2, respectively. Compared with the K_w determined by the single-porosity model in Table 1, the calculated ones are much lower.

The volumetric fraction factor w_f represents the portion of the total pore volume occupied by large pores. It can be used to calculate the total water content or degree of saturation, but it is different from the transport contribution factor of each porosity region. According to the classical theories for permeability [49,50], permeability is not a linear function of the pore size, but a square function. This indicates that large pores have the higher permeability than the small pores even though they have the same volumetric fraction. This also indicates that the transport contribution factor of large pores should be much greater than w_f. Hence, in regard to calculating K_w, the use of w_f as in Eq. (15) instead of the actual contribution to moisture transport can significantly underestimate the results.

5.4 Microstructural effect of drying and wetting

In addition to the dual-porosity property, the microstructural changes during drying or wetting may be another reason for anomalous moisture transport. In an ESEM study, Fonseca and Jennings [51] found that if a specimen is dried at a given RH (not directly to zero-RH) the morphology of hydration products at the microscale is altered as a solid layer over C-S-H needles appears. After comparing different water removal methods, Zhang et al. [40] found that all drying methods can change the morphology of C-S-H to varying degrees. For instance, C-S-H fibers totally fall onto the cement grains for a harsh drying method (e.g., drying direct from water), while for a gentle drying approach (e.g., isopropanol replacement or supercritical drying), a thin film is created between two C-S-H fibers. By observing the *in situ* rehydration of the dried cement paste by an ESEM, Hall et al. [12] found that the paste size was enlarged after it adsorbed water. The comparison of the pore size distributions measured by MIP for the dried sample and by NMR for the resaturated sample shows that PSD peaks for the resaturated sample shift to the finer pore range [18], indicating that the resaturated sample was swelling. In summary, the morphological change of C-S-H during drying and wetting is illustrated by Fig. 10. After drying, the original needle-like structure partially collapses, which is recovered to a certain extent by rewetting, but cannot reach the same level as the original structure. Macroscopically, this is proved by the measured sorption isotherms [52] which show after the desorption-adsorption cycles that the total water content of the resaturated sample is lower than that of the saturated sample before measurement, indicating that the total porosity is smaller after the desorption-adsorption cycles.

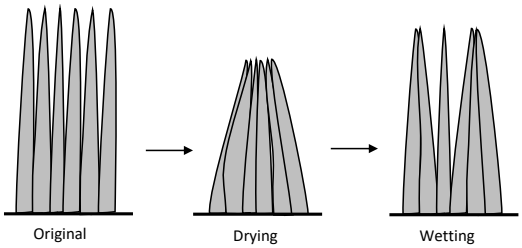

Fig. 10 Effects of drying and wetting on the morphology of hydration products. Drying results in the collapse of needle-like structures and only partial structures can be recovered after wetting.

All these morphological effects directly change the characteristics of micropores, such as pore structures, connectivity, etc. Consequently, the moisture transport properties are expected to be different from what we use in the proposed dual-permeability model. However, the microstructural alterations during drying or wetting are difficult to be quantified, so that the effect cannot be accurately considered in the proposed dual-permeability model.

5.5 Multi-porosity concept

While considering the concept of two-porosity still presents a simplification of the complex pore network, we find that this approach can significantly improve the prediction of moisture transport in cement pastes, in particular for the case so-called anomalous moisture transport. To further consider the complexity of the pore network, a multi-porosity model can be developed based on the concept of multi-porosity [53]. For cement pastes studied in this paper, the dual-porosity is sufficient enough to provide accurate fittings. But for uncracked concrete, the additional porosity may be added from the interracial transition zone (ITZ) around aggregates because it is well-known that the porosity of this zone is lower than the bulk concrete [54,55,6]. The volumetric fraction of ITZ could be estimated based on the volume of aggregates and the assumed ITZ width [56]. For cracked concrete, the cracks can be separated as a porosity region [33]. However, more porosity regions will lead to more parameters in the model to be fitted by experimental data. This will need much more experimental data which will largely decrease model's robustness.

6 Conclusion

Cement-based materials have a complex porosity with pore sizes spanning from the nanometer to the millimetter rang. Nevertheless, conventional approaches to model transport processes through the pore system are based on the single-porosity concept and sometimes fail to accurately describe experimental results. The present study proposes a dual-permeability model to better knowledge moisture transport in the complex pore system in cementitous materials. The model considers the contribution of both liquid water and water vapor to moisture transport. From the experimental validation, the following major conclusions can be drawn:

1. The dual-permeability model can well simulate the anomalous mass change curves for cement paste specimens dried/wetted at different RHs, while the single-porosity model finds poor agreement with the experimental data.
2. The applicability of the proposed dual-permeability model suggests that the "dual-porosity property" could be one of the reasons that lead to anomalous moisture transport in cement pastes.
3. Vapor diffusion in either large or small pores is not negligible for moisture transport in the RH range below the demarcation point (the separation point between the liquid transport and vapor diffusion dominant regions) in the apparent diffusivity curve.
4. We found that when the moisture transfer factor ξ is smaller than a certain value (depending on the material), ξ becomes less sensitive. In this study, ξ = 1E-3 kg/s/m^3 works for all materials.
5. The volumetric fraction of each porosity region determined by fitting the measured sorption isotherm with a bimodal equation works well in the dual-permeability model.
6. However, the use of the volumetric fraction to calculate the overall permeability (which is commonly found in the literature) largely underestimates the results. This suggests that the volumetric fraction is different from the transport contribution factor that should be used for the determination of permeability.
7. When fitting the anomalous mass change curves, we could not find close values of permeability for different drying (or wetting) conditions. Therefore, the development of a universal dual-permeability model for anomalous moisture transport needs to consider more factors, such as chemical interactions of water with hydration products and the microstructural changes during drying/wetting.

Funding

The research was funded by the Swiss National Science Foundation (SNSF) through the ENDURE project (grant number PP00P2-163675).

Compliance with ethical standards

Conflict of interest

The authors have no conflict of interest to declare.

References

1. V. Baroghel-Bouny, M. Thiery, M. Dierkens, and X. Wang, "Aging and durability of concrete in lab and in field conditions–pore structure and moisture content gradients between inner and surface zones in rc structural elements," *Journal of Sustainable Cement-Based Materials*, vol. 6, no. 3, pp. 149–194, 2017.
2. L.-O. Nilsson, "Water and the hygro-thermal characteristics of hardened concrete," (St-Remy-les-Chevreuse, France), FNB-Collège International des Sciences de la Construction, pages 122 - 138, 1985.
3. Q.-f. Liu, G.-l. Feng, J. Xia, J. Yang, and L.-y. Li, "Ionic transport features in concrete composites containing various shaped aggregates: a numerical study," *Composite Structures*, vol. 183, pp. 371–380, 2018.

4. V. Baroghel-Bouny, X. Wang, M. Thiéry, M. Saillio, and F. Barberon, "Prediction of chloride binding isotherms of cementitious materials by analytical model or numerical inverse analysis," *Cement and Concrete Research*, vol. 42, pp. 1207–1224, 2012.
5. L.-x. Mao, Z. Hu, J. Xia, G.-l. Feng, I. Azim, J. Yang, and Q.-f. Liu, "Multi-phase modelling of electrochemical rehabilitation for asr and chloride affected concrete composites," *Composite Structures*, vol. 207, pp. 176–189, 2019.
6. Z. Zhang, U. Angst, A. Michel, and M. Jensen, "An image-based local homogenization method to model mass transport at the steel-concrete interface," in *Sixth International Conference on the Durability of Concrete Structures* (P.A.M.Basheer, ed.), (Leeds, UK), pp. 807–814, Whittles Publishing, 2018.
7. U. M. Angst, "Challenges and opportunities in corrosion of steel in concrete," *Materials and Structures*, vol. 51, p. 4, 2018.
8. Z. P. Bazant and L. J. Najjar, "Nonlinear water diffusion in non-saturated concrete," *Material and Structure*, vol. 25, pp. 3–20, 1972.
9. O. Coussy, *Mechanics of porous continua*. New York: Wiley, 1995.
10. M. Mainguy, O. Coussy, and V. Baroghel-Bouny, "Role of air pressure in drying of weakly permeable materials," *Journal of Engineering Mechanics*, vol. 127, pp. 582–592, 2001.
11. L. Wadsö, "A critical review on anomalous or non-fickian vapor sorption," tech. rep., Rapport TVBM (Intern 7000-rapport); Vol. 7017. Division of Building Materials, LTH, Lund University, Sweden, 1992.
12. C. Hall, W. Hoff, S. Taylor, M. Wilson, B.-G. Yoon, H.-W. Reinhardt, M. Sosoro, P. Meredith, and A. Donald, "Water anomaly in capillary liquid absorption by cement-based materials," *Journal of Materials Science Letters*, vol. 14, no. 17, pp. 1178–1181, 1995.
13. S. Taylor, W. Hoff, M. Wilson, and K. Green, "Anomalous water transport properties of portland and blended cement-based materials," *Journal of materials science letters*, vol. 18, no. 23, pp. 1925–1927, 1999.
14. M. Saeidpour and L. Wadsö, "Evidence for anomalous water vapor sorption kinetics in cement based materials," *Cement and Concrete Research*, vol. 70, pp. 60–66, 2015.
15. S. Mindess and J. Young, *Concrete*. Upper Saddle River, NJ, USA: Prentice Hall, 1981.
16. Z. Zhang, M. Thiery, and V. Baroghel-Bouny, "An equation for drying kinetics of cementitious materials," *Drying Technology*, vol. 36, pp. 1446–1459, 2018.
17. Q. Zeng and S. Xu, "A two-parameter stretched exponential function for dynamic water vapor sorption of cement-based porous materials," *Materials and Structures*, vol. 50, p. 128, 2017.
18. C. Zhou, F. Ren, Z. Wang, W. Chen, and W. Wang, "Why permeability to water is anomalously lower than that to many other fluids for cement-based material?," *Cement and Concrete Research*, vol. 100, pp. 373–384, 2017.
19. Z. Zhang, M. Thiery, and V. Baroghel-Bouny, "Numerical modelling of moisture transfers with hysteresis within cementitious materials: Verification and investigation of the effects of repeated wetting–drying boundary conditions," *Cement and Concrete Research*, vol. 68, pp. 10–23, 2015.
20. G. Barenblatt, I. P. Zheltov, and I. Kochina, "Basic concepts in the theory of seepage of homogeneous liquids in fissured rocks [strata]," *Journal of applied mathematics and mechanics*, vol. 24, no. 5, pp. 1286–1303, 1960.
21. J. Warren and P. J. Root, "The behavior of naturally fractured reservoirs," *SPE Journal*, pp. 245–255, 1963.
22. R. W. Zimmerman, G. Chen, T. Hadgu, and G. S. Bodvarsson, "A numerical dual-porosity model with semianalytical treatment of fracture/matrix flow," *Water resources research*, vol. 29, no. 7, pp. 2127–2137, 1993.
23. Z.-X. Chen, "Transient flow of slightly compressible fluids through double-porosity, double-permeability systems—a state-of-the-art review," *Transport in Porous Media*, vol. 4, no. 2, pp. 147–184, 1989.
24. R. Wallach, O. Troygot, and I. Saguy, "Modeling rehydration of porous food materials: II. The dual porosity approach," *Journal of Food Engineering*, vol. 105, pp. 416–421, 2011.
25. S. Nikoosokhan, M. Vandamme, and P. Dangla, "A poromechanical model for coal seams injected with carbon dioxide: From an isotherm of adsorption to a swelling of the reservoir," *Oil & Gas Science and Technology*, vol. 67, pp. 777 – 786, 2012.
26. H.H.Gerke and M. T. van Genuchten, "Evaluation of a first-order water transfer term for variably saturated dual-porosity flow models," *Water Resources Research*, vol. 29, pp. 1225–1238, 1993.

27. H.H.Gerke and M. T. van Genuchten, "A dual-porosity model for simulating the preferential movement of water and solutes in structured porous media," *Water Resources Research*, vol. 29, pp. 305–319, 1993.
28. M. T. van Genuchten, "A closed-form equation for predicting the hydraulic conductivity of unsaturated soils," *Soil Science Society of America Journal*, vol. 44, pp. 892–898, 1980.
29. Y. Mualem, "A new model for predicting the hydraulic conductivity of unsaturated porous media," *Water Resources Research*, vol. 12, pp. 513–522, 1976.
30. J. M. Köhne, S. Köhne, and H. H. Gerke, "Estimating the hydraulic functions of dual-permeability models from bulk soil data," *Water Resources Research*, vol. 38, no. 7, pp. 261–2611, 2002.
31. J. M. Köhne, B. P. Mohanty, and J. Šimůnek, "Inverse Dual-Permeability Modeling of Preferential Water Flow in a Soil Column and Implications for Field-Scale Solute Transport," *Vadose Zone Journal*, vol. 5, no. 1, p. 59, 2006.
32. D. Ma and M. Shao, "Simulating infiltration into stony soils with a dual-porosity model," *European Journal of Soil Science*, vol. 59, no. 5, pp. 950–959, 2008.
33. D. Smyl, F. Ghasemzadeh, and M. Pour-Ghaz, "Can the dual-permeability model be used to simulate unsaturated moisture flow in damaged mortar and concrete?," *International Journal of Advances in Engineering Sciences and Applied Mathematics*, vol. 9, no. 2, pp. 54–66, 2017.
34. J. Carlier and N. Burlion, "Experimental and Numerical Assessment of the Hydrodynamical Properties of Cementitious Materials," *Transport in Porous Media*, vol. 86, no. 1, pp. 87–102, 2011.
35. Z. Zhang, M. Thiery, and V. Baroghel-Bouny, "A review and statistical study of existing hysteresis models for cementitious materials," *Cement and Concrete Research*, vol. 57, pp. 44–60, 2014.
36. W. Durner, "Hydraulic conductivity estimation for soils with heterogeneous pore structure," *Water Resources Research*, vol. 30, p. 211–233, 1994.
37. Z. Zhang, *Modelling of sorption hysteresis and its effect on moisture transport within cementitious materials*. PhD thesis, Université Paris-Est, 2014.
38. B. Berkowitz, J. Bear, and C. Braester, "Continuum models for contaminant transport in fractured porous formations," *Water Resources Research*, vol. 24, no. 8, pp. 1225–1236, 1988.
39. J. Kodikara, S. Barbour, D. Fredlund, *et al.*, "Changes in clay structure and behaviour due to wetting and drying," in *Proceedings 8th Australia New Zealand Conference on Geomechanics: Consolidating Knowledge*, p. 179, Australian Geomechanics Society, 1999.
40. Z. Zhang, G. W. Scherer, and A. Bauer, "Morphology of cementitious material during early hydration," *Cement and Concrete Research*, vol. 107, pp. 85–100, 2018.
41. O. Ippisch, H.-J. Vogel, and P. Bastian, "Validity limits for the van genuchten-mualem model and implications for parameter estimation and numerical simulation," *Advances in Water Resources*, vol. 29, pp. 1780–1789, 2006.
42. V. Baroghel-Bouny, "Water vapour sorption experiments on hardened cementitious materials. Part II: Essential tool for assessment of transport properties and for durability prediction," *Cement and Concrete Research*, vol. 37, pp. 438–454, 2007.
43. R. Millington and J. Quirk, "Permeability of porous solids," *Transactions of the Faraday Society*, vol. 57, pp. 1200–1207, 1961.
44. M. Thiéry, P. Belin, V. Baroghel-Bouny, and M. D. Nguyen, "Modelling of isothermal drying process in cementitious materials – Analysis of the moisture transfer and proposal of simplified approaches," in *Proceedings of 3rd International Conference on Coupled T-H-M-C Processes in Geo-systems*, (Polytech Lille, France), pp. 571–581, 2008.
45. V. Baroghel-Bouny, "Water vapour sorption experiments on hardened cementitious materials. Part I: Essential tool for analysis of hygral behaviour and its relation to pore structure," *Cement and Concrete Research*, vol. 37, no. 3, pp. 414 – 437, 2007.
46. M. T. Nguyen, *Modélisation des couplages entre hydratation et dessiccation des matériaux cimentaires à l'issue du décoffrage*. PhD thesis, ENPC, September 2009.
47. M. Wu, *Using low temperature calorimetry and moisture fixation method to study the pore structure of cement based materials*. PhD thesis, Technical University of Denmark, September 2014.
48. M. Saeidpour and L. Wadsö, "Moisture equilibrium of cement based materials containing slag or silica fume and exposed to repeated sorption cycles," *Cement and Concrete Research*, vol. 69, p. 88095, 2015.

49. R. Millington and J. Quirk, "Permeability of porous solids," *Transactions of the Faraday Society*, vol. 57, pp. 1200–1207, 1961.
50. A. Katz and A. Thompson, "Prediction of rock electrical conductivity from mercury injection measurements," *Journal of Geophysical Research: Solid Earth*, vol. 92, no. B1, pp. 599–607, 1987.
51. P. Fonseca and H. Jennings, "The effect of drying on early-age morphology of C–S–H as observed in environmental SEM," *Cement and Concrete Research*, vol. 40, pp. 1673–1680, 2010.
52. M. Wu, B. Johannesson, and M. Geiker, "A study of the water vapor sorption isotherms of hardened cement pastes: Possible pore structure changes at low relative humidity and the impact of temperature on isotherms," *Cement and Concrete Research*, vol. 56, pp. 97–105, 2014.
53. E. Aifantis, "Introducing a multi-porous medium," *Dev. Mech*, vol. 8, no. 37, pp. 209–211, 1977.
54. J. Ollivier, J. Maso, and B. Bourdette, "Interfacial transition zone in concrete," *Advanced cement based materials*, vol. 2, no. 1, pp. 30–38, 1995.
55. K. L. Scrivener, A. K. Crumbie, and P. Laugesen, "The interfacial transition zone (ITZ) between cement paste and aggregate in concrete," *Interface Science*, vol. 12, no. 4, pp. 411–421, 2004.
56. E. J. Garboczi and D. P. Bentz, "Analytical formulas for interfacial transition zone properties," *Advanced Cement Based Materials*, vol. 6, no. 3-4, pp. 99–108, 1997.